Solution structure of human CTLA-4 and delineation of a CD80/CD86 binding site conserved in CD28

The structure of human CTLA-4 reveals that residues Met 99, Tyr 100 and Tyr 104 of the $M_{99}YPPPY_{104}$ motif are adjacent to a patch of charged surface residues on the A'GFCC' face of the protein. Mutation of these residues, which are conserved in the CTLA-4/CD28 family, significantly reduces binding to CD80 and/or CD86, implicating this patch as a ligand binding site.

Cytotoxic T Lymphocyte–Associated Protein-4 (CTLA-4 or CD152) and CD28 are homologous T-lymphocyte receptors which bind common ligands (CD80 and CD86), but have distinct functions during an immune response[1]. CD28 engagement stimulates production of interleukin-2 and other T-cell cytokines which are essential for effective T-cell proliferation[1]. CTLA-4, on the other hand, negatively regulates T-cell activation[2–5], and mice deficient for this molecule exhibit a severe lymphoproliferative disorder and early lethality[6–7]. CTLA-4 binds CD80 and CD86 with >500-fold higher avidity than does CD28[8]. Covalent dimerization of CTLA-4 is required for its high binding avidity, but each monomeric subunit contains a binding site for CD80 and CD86[9]. A soluble immunoglobulin (Ig) fusion protein of CTLA-4 (CTLA4Ig) blocks T cell co-stimulation through CD28[10], and is immunosuppressive in *in vivo* models of autoimmune diseases and organ graft rejection[11].

We have determined the solution structure of CTLA-4ex, an extracellular fragment of human CTLA-4 by multidimensional, heteronuclear NMR spectroscopy (Fig. 1, Table 1). Although CTLA-4 occurs as a disulphide-linked dimer *in vivo*, we found no evidence for association of monomeric subunits of CTLA-4ex into dimers under the conditions of the NMR experiments. A rotational correlation time of 8.2 ± 0.2 ns was estimated from the ratio of ^1H_N T_1 and T_2 relaxation times, consistent with previous biochemical studies suggesting that, in the absence of the disulphide, CTLA-4 was monomeric in solution[8]. The structure of CTLA-4ex is most similar to immuno-globulin superfamily variable–domains (IgSVF). In CTLA-4ex, the two β-sheets of the V-fold comprise the ABED and A'GFCC' strands,

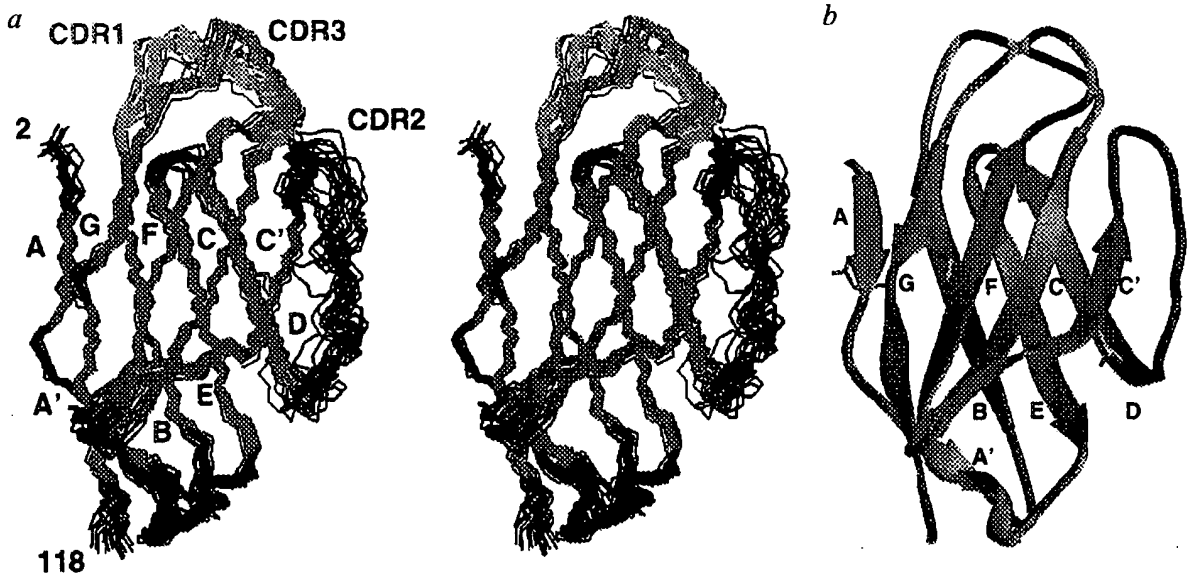

Fig. 1 Structure of CTLA-4ex. ***a***, The 20 structures representing the NMR ensemble. The structures were superimposed for the best fit of the backbone (N, Cα, C') atoms of the residues 2–54, and 68–118 to the average structure. The first two N-terminal residues and the last 13 C-terminal residues are ill-defined structurally and are not shown. The structures are coloured as in (*b*). ***b***, Ribbon diagram[27] depicting the secondary structure: β-strands A (residues Thr 4–Pro 6), A' (Val 9–Ala 11), B (Ile 17–Tyr 23), C (Val 32–Ala 40), C' (Gln 43–Ala 50), D (Ile 67–Ser 73), E (Gln 76–Gln 82), F (Gly 90–Glu 97) and G (Gly 108–Gly 110,Gly 112–Tyr 116) form two β-pleated sheets — strands ADEB are blue and A'GFCC' are red — that adopt a β-sandwich conformation. Strands C and C' are joined by a type 1 β-turn (Ala 40–Gln 43); Strands D and E by a type II' β-turn; and strands E and F by one 3_{10}-helical turn (Ala 86–Asp 88). Also highlighted are the CDR1 (green) and CDR3 (magenta) analogous loops, the disulphide bonds (yellow), and Asn 111 (orange). The second glycosylation site, Asn 78, is hidden in this orientation behind strand E.

respectively, which are connected by two disulphide bonds, the canonical Ig-disulphide (Cys 21–94) and an additional non-Ig disulphide bond (Cys 48–68). CTLA-4ex contains two N-linked glycosylation sites (Asn 78 and Asn 111). After partial deglycosylation, both of these residues carry the glycans, mannose-β1→4-N-acetylglucosamine-β1→4-(α1→6-fucose) N-acetylglucosamine.

The Asn 78 glycan interacts extensively with the side chains of residues on the DEB face of CTLA-4ex. Numerous nuclear Overhauser effects (NOEs) were observed between the N-acetylglucosamine (GlcNac) and fucose protons, and protein residues in three different strands: Ile 16, Ser 18, and Val 20 (strand B); Thr 71 (strand D); and Thr 80 (strand E). These intimate protein–carbohydrate interactions are reminiscent of CD2[12], where an N-linked glycan also shows NOEs with residues in several β-strands. In CD2, the carbohydrate counterbalances a high local concentration of positively charged residues[12], but the DEB surface of CTLA-4ex does not contain such a basic patch. The Asn 78 glycosylation is completly conserved in CTLA-4, but not CD28, homologues (Fig. 2*a*). Mutation of Asn 78 in CTLA4Ig leads to protein aggregation, which is accompanied by a reduction in binding activity (Table 2), suggesting that glycosylation at Asn 78 is important for structural integrity and/or solubility of CTLA-4.

Table 1 Structural Statistics of CTLA-4ex

R.m.s.d.[1]	
residues 2–118 (N, Cα, C')[1]	0.83 Å
residues 2–54, 68–118 (N, Cα, C')[1]	0.69 Å
residues 2–118 (non-hydrogens)	1.26 Å
residues 2–54, 68–118 (non-hydrogens)	1.07 Å
residues 2–118 and ordered sugar residues (non-hydrogens) [2]	1.31 Å
Deviations from experimental restraints[3]	
r.m.s.d. of NOE restraints (Å)	0.055 ± 0.003
largest NOE violation[4] (Å)	0.49
# NOE violations > 0.4 Å	3.2 ± 1.2
# NOE violations > 0.3 Å	9.7 ± 2.1
r.m.s.d. of Φ and χ_1 torsion restraints (°)	0.27 ± 0.14
largest torsion angle violation[4] (°)	2.4
Deviations from idealized covalent geometry	
r.m.s.d. of bond lengths (Å)	0.010 ± 9e-4
r.m.s.d. of bond angles (°)	1.34 ± 0.04
r.m.s.d. of improper angles (°)	1.60 ± 1.08
Energies[5]	
E(NOE)	144 ± 16
E(cdih)	16.1 ± 17.2
E(L-J)	-379 ± 76

[1]The r.m.s.d. listed is the average root-mean-squared distance deviation obtained after superposition of each individual structure on the average structure.
[2]Four sugars were included in the calculation: the two GlcNac and fucose residues attached at Asn 78, and the N-linked GlcNac attached at Asn 111.
[3]All deviations are represented as the average ± 1 standard deviation and are calculated for the ensemble of 20 CTLA-4ex structures.
[4]The largest individual NOE or torsion angle restraint violation in any of the 20 refined structures is listed.
[5]Energies are calculated with X-PLOR using the parallhdg_new.pro and param3_mod.cho parameter sets, and are reported in units of kcal mol^{-1}. E(NOE) and E(cdih) were calculated with a square-well quadratic potential with force constants of 50 kcal mol^{-1} $Å^{-2}$ and 200 kcal mol^{-1} rad^{-2}, respectively. E(L-J), the Leonard-Jones van der Waals energy calculated with the X-PLOR empirical energy function, was not used during structure refinement. In addition, a quartic van der Waals repulsion function was included. The force constant on the NOE restraints and torsion angle restraints were set to 50 kcal mol^{-1} $Å^{-2}$ and 50 kcal mol^{-1} rad^{-2} respectively.

In contrast, limited interactions were detected between the protein residues and the Asn 111 glycan. NOEs were only observed be-tween the N-linked GlcNac H1, H2 and N-acetyl methyl group, and protein residues Ile 93 and Ile 109. Thus, this GlcNac is the only conformationally well-defined sugar residue attached to Asn 111. The Asn 111 glycan is accomodated by the β-bulge in the G strand. The Asn111Asp mutation of CTLA4Ig did not detectably affect binding activity to CD80 and CD86 (Table 2), indicating that the glycan is not essential for binding or maintaining protein solubility. This result is surprising in light of the rigorous conservation of the Asn 111 glycosylation site in all CTLA-4 and CD28 homologues (Fig. 2*a*).

CTLA-4 is a disulphide-linked homodimer. In binding studies with CD80 and CD86, the CTLA-4 dimer was found to have a much slower off rate relative to monomeric CTLA-4, reflecting the higher avidity of the dimer (there are two binding sites per dimer)[8]. The spacing of six residues between the end of Ig fold (Val 117) and the cysteine involved in homodimerization (Cys 123) could provide sufficient rotational freedom for the two subunits of a CTLA-4 dimer to adopt many possible orientations. Although we have no direct physical evidence for or against a preferred orientation of the monomeric subunits in the disulphide-linked dimer, indirect evidence argues against certain orientations. The possible modes of dimerization are limited by the N-linked glycans. Dimerization of subunits along the G strands would be sterically restricted by the Asn 111 glycan. Dimerization involving the ABED face would be also be sterically restricted by glycan at Asn 78. In antibodies and CD8, dimerization is mediated through the A'GFCC' face[13]. Several structural features would argue against this mode of dimerization in CTLA-4. First, residues in the CDR1- and CDR3-analogous loops interact, which results in a reduction of curvature of the F and G strands, and excludes a number of the stabilizing dimerization contacts found in antibodies. Second, of the two β-bulges involved in Fv-like dimerization[13], only the G strand β-bulge is present in CTLA-4ex; the β-bulge immediately N-terminal to the C' strand is absent. Third, the A'GFCC' face in CTLA-4ex is not distinctly hydrophobic, but contains several charged residues (Fig. 2). Finally, residue Ile 109 in CTLA-4ex, which corresponds to a residue involved in dimerization of Fv fragments, interacts with the Asn 111 glycan. These structural features suggest that the A'GFCC' face of CTLA-4ex has evolved to serve a different function than that of the corresponding face in antibodies. One potential dimerization interface of the subunits could involve parts of the A'B and G strands that are conserved in CTLA-4 but not in CD28. This region is located between the two N-linked glycans and forms a coherent surface. However, if there is a preferred orientation of the subunits in the dimer, the interactions between these subunits must be weak, since CTLA-4ex is monomeric in solution.

The hexapeptide MYPPPY motif in the F–G loop (CDR3-analogous region) is conserved in CTLA-4 and CD28, and is essential for ligand binding. Mutation of any of these residues in CTLA-4 or CD28 leads to reduced binding of CD80 and/or CD86[14–17] (Table 2). In CTLA-4ex, this motif forms a loop that is conformationally restrained due to the presence of three consecutive prolines, the last of which, Pro 103, is in the *cis* conformation (see Methods). The loop is stabilized by a

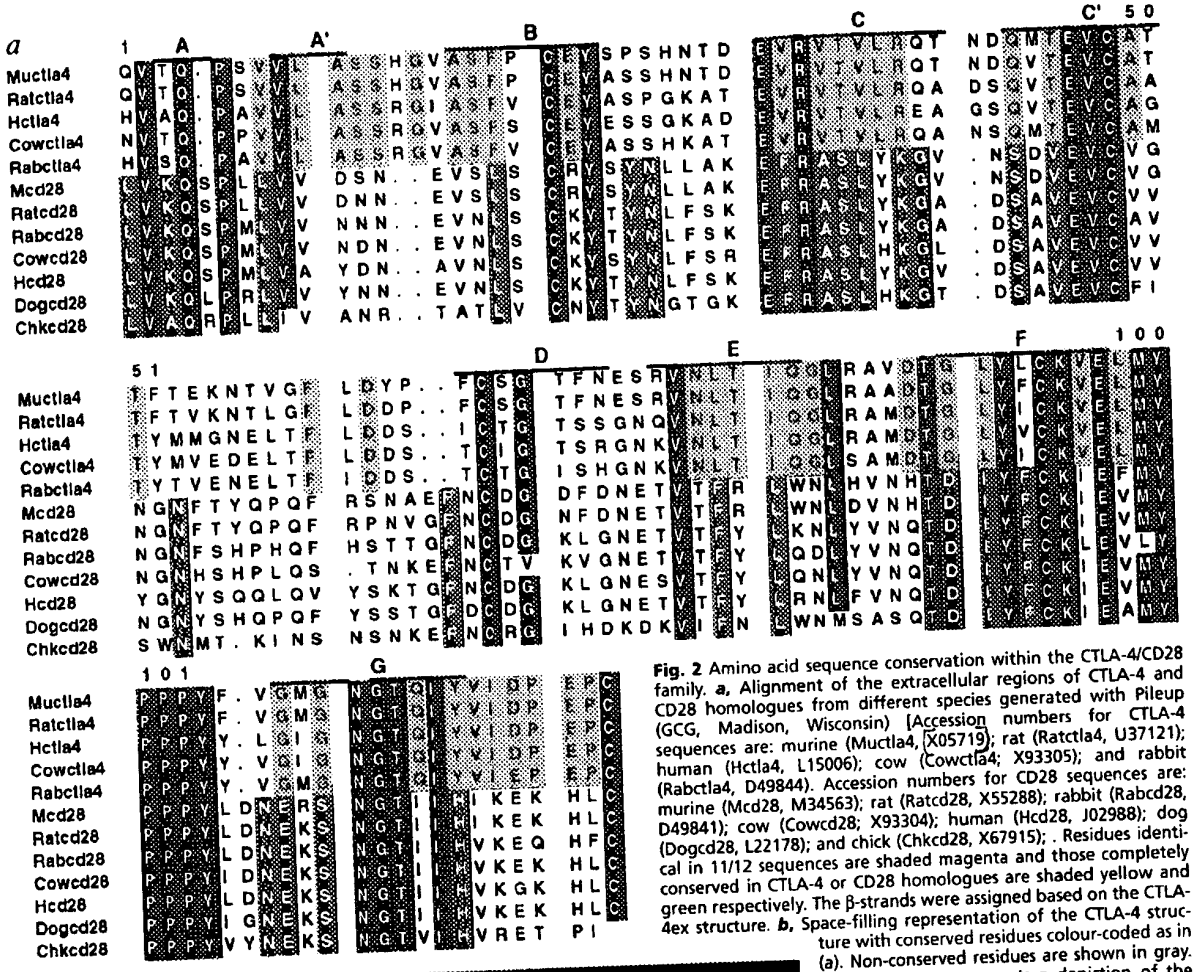

Fig. 2 Amino acid sequence conservation within the CTLA-4/CD28 family. ***a***, Alignment of the extracellular regions of CTLA-4 and CD28 homologues from different species generated with Pileup (GCG, Madison, Wisconsin) [Accession numbers for CTLA-4 sequences are: murine (Muctla4, X05719); rat (Ratctla4, U37121); human (Hctla4, L15006); cow (Cowctla4; X93305); and rabbit (Rabctla4, D49844). Accession numbers for CD28 sequences are: murine (Mcd28, M34563); rat (Ratcd28, X55288); rabbit (Rabcd28, D49841); cow (Cowcd28; X93304); human (Hcd28, J02988); dog (Dogcd28, L22178); and chick (Chkcd28, X67915); . Residues identical in 11/12 sequences are shaded magenta and those completely conserved in CTLA-4 or CD28 homologues are shaded yellow and green respectively. The β-strands were assigned based on the CTLA-4ex structure. ***b***, Space-filling representation of the CTLA-4ex structure with conserved residues colour-coded as in (a). Non-conserved residues are shown in gray. The left image represents a depiction of the A'GFCC' face; this was rotated −180° around the vertical axis to obtain the right image, which is a depiction of the BED face. Glycosylated asparagines are shaded blue. A number of highly conserved surface residues have been labelled.

hydrogen bond between the Pro 101 O and the Tyr 104 H_N. The conformation of the MYPPPY loop places Met 99, Tyr 100, and Tyr 104 on the A'GFCC' β-sheet surface. In contrast, both Leu 98 and Leu 106 point in the opposite direction and pack closely against Tyr 23 and Ser 25 of the CDR1-analogous loop. The conformation of the MYPPPY loop extends the A'GFCC' face by making the β-sheet surface flatter than usually found in IgSF V-domains, and in combination with the absence of Fv-like dimerization, provides a large accessible surface suitable for mediating binding interactions.

The binding of common ligands by CTLA-4 and CD28 suggests that their binding sites should overlap and include conserved residues. Sequence conservation within the CTLA-4/CD28 family was determined by an amino acid sequence alignment of the extracellular regions (Fig. 2*a*). While sequence conservation was scattered throughout the primary structure, many of the conserved residues clustered spatially (Fig. 2*b*). When conserved residues were mapped on the CTLA-4ex structure, the BED face showed

little sequence conservation (Fig. 2*b*), especially in the vicinity of the non-Ig disulphide bond (Cys 48–68) and the glycosylation site at Asn 78 . Thus, while the non-Ig disulphide bond is completely conserved in the CTLA-4/CD28 family, the intervening residues show the least conservation within the family. The lack of sequence conservation in this region suggested that the BED face is not involved in ligand binding. Consistent with this, simultaneous mutation of several adjacent residues on the BED face of CD28 did not affect ligand binding (Table 2).

Table 2 Effects of mutations of CTLA-4 on CD80 and CD86 ligand binding

Location of mutation	Mutation	CD80	CD86
	Wild type	+	+
Glycosylation site	N78D	-#	-#
Glycosylation site	N111D	+	+
A'GFCC' face	E31S	-	-
A'GFCC' face	R33S	-/+	-
A'GFCC' face	T35S	+	+
A'GFCC' face	L37S	+	+
A'GFCC' face	E46S	+/-	-
A'GFCC' face	T51S	+	+
A'GFCC' face	K95S	-	-

Listed are the effects of mutations of residues of CTLA-4 on CD80 and CD86 ligand binding. Mutations which substantially reduced binding to either CD80 or CD86 (that is, binding reduced by >80%, compared to wild type CTLA4Ig) are depicted as - ; mutations which had little effect on binding (that is, binding reduced by <20%) are depicted as +. #, This mutation led to significant aggregation of CTLA-4.
Other CTLA-4 (¥) or CD28 (§) mutations that were shown previously to affect binding to CD80 or CD86 include: KE(95,97)AA[¥15]; M99A[¥14]; Y100A[¥14]; P101A[¥14]; P102A[¥14]; P103A[¥14,16]; Y104A[¥§14,16]; MYPPPY(99-104)SGGG[§16–17]; YP(100,102)LG[§16]; PP(101,103)GL[§16]; YY(100,104)FF[§17]; YLD(104-106)LAS[§16]. Other mutations that were shown previously to have no affect on binding include: K14A[¥15], EY(22-23)AF[¥15]; YSQ(54-56)FTY[§16]; SQQ(55-57)ATS[§16]; KLG(71-73)DFD[§16].

In contrast, the A'GFCC' face, extended by the MYPPPY loop, contains a patch of residues conserved in both CTLA-4 and CD28 (Fig. 2*b*). Included in this patch are residues comprising the hydrophobic MYPPPY loop in close proximity to a number of charged residues (Glu 31, Arg 33, Glu 46, Lys 95 and Glu 97). This juxtaposition of conserved hydrophobic and charged residues makes this an attractive candidate ligand binding site of CTLA-4ex. This hypothesis is substantiated by site-specific mutagenesis experiments. Mutations of most of the residues in the conserved surface patch on the A'GFCC' face abolish binding to CD80 and/or CD86 (Table 2). Several of these mutations, such as Arg33Ser and Glu46Ser, affected CTLA-4 binding to CD86 more than to CD80. Another example of this is the conservative Tyr100Phe mutation of CTLA4Ig, which abolishes CTLA4Ig binding to CD86 without affecting binding to CD80[18]. Thus, an overlapping but non-identical set of residues on the A'GFCC' face of CTLA-4 determine binding to CD80 and CD86.

In the absence of three-dimensional structures of the CTLA-4 mutant proteins, we cannot rule out completely the possibility that their reduced CD80/CD86 binding is caused by alterations in their backbone conformations. However, several lines of evidence suggest that the mutant proteins adopt the native fold, and that the reduced CD80/CD86 binding is due to altered interactions with the side chains of the CTLA-4 mutants. First, all mutations listed in Table 2 result in proteins that are bound by a panel of monoclonal antibodies that bind native CTLA-4. Second, certain mutations selectively affect either CD80 or CD86 binding, suggesting that the effects of the mutations are due to specific interactions. In addition to the CTLA-4 mutants described above, Tyr100Phe and Tyr104Phe mutations in CD28 also selectively perturbed binding to CD86[17]. Furthermore, at high concentrations, several Ala mutants of the MYPPPY motif retained binding activity to CD80 (but not CD86)[14–15]. Finally, the mutants occupy surface positions in CTLA-4 structure, and thus are not expected to significantly perturb the structure.

The identification of a CTLA-4ex ligand binding site sheds new light on one of the key biological properties of the CTLA-4 receptor, its high avidity for CD80 and CD86 ligands. Homologue mutagenesis studies showed that the binding avidity of CD28 was increased by replacement of segments from the G strand and B–C loop (CDR-1 analogous region) with the corresponding regions from CTLA-4[14]. Neither of these sequences is well conserved between CTLA-4 and CD28 (Fig. 2*a*); the G strand, in particular, is distinctly different in both length and charge between the two molecules. The CTLA-4ex structure shows that the G strand and B–C loop are spatially adjacent to the conserved ligand binding site. Residues in the N-terminal portion of the G strand extend to one side of the conserved surface patch in CTLA-4ex, whereas the C-terminal section of the B-C loop extends to the other. Thus, the structure suggests that non-conserved residues peripheral to a conserved central binding site modulate the binding characteristics of the CTLA-4/CD28 receptor family, and may contribute to the different biological properties of these receptors.

Methods

Sample Preparation. CTLA4Ig, a soluble fusion protein of the immunoglobulin Cγ1 chain with the extracellular domain of human CTLA-4[10], was expressed by a Chinese hamster ovary (CHO) cell line and was purified from the culture medium by Protein-A chromatography[10]. Dimeric CTLA-4t dimer was prepared as described[9]. CTLA-4ex monomer was obtained by reduction of the interchain disulphide in CTLA-4t by 1 mM DTT followed by iodoacetamide modification of the free sulphydryl and ion-exchange chromatography on a Resource-Q (Pharmacia) column. The two N-linked carbohydrates on each monomer were nominally converted to a tetrasaccharide core (complete deglycosylation of CTLA-4ex results in protein aggregates at concentrations under which the NMR experiments were performed.) by treatment with *Arthobacter. ureafaciens* sialidase, *Streptococcus pneumoniae* β-galactosidase, jack bean β-N-acetylhexosaminidase and jack bean α-mannosidase (Oxford Glycosystems) in 100 mM NaAc, 2 mM ZnCl2, pH 5. The sample was then dialyzed into 25 mM deuterated Tris-maleate, 0.1 mM EDTA, 0.1 mM NaN_3, 7% D_2O, pH 7.03, and concentrated to 0.7 mM. After trimming the carbohydrate with the cocktail of enzymes, we estimated that ~30 heterogeneity existed in the carbohydrate. We were unable to detect this heterogeneity in the NMR as resonances from the terminal mannoses were overlapped. All of this heterogeneity appears to be the result of an additional mannose attached to the remaining tetrasaccharide core at either N111 and/or N78 (as determined by mass spectroscopy, gel filtration, and carbohydrate analysis; unpublished results). The resulting partially deglycosylated CTLA-4ex was as active as fully glycosylated CTLA-4ex by ELISA CD80 binding inhibition assay. For multidimensional NMR experiments, CHO cell-produced CTLA4Ig was labelled with ^{15}N and ^{13}C by growth in Select-Amine media (Gibco) containing all $^{15}N/^{13}C$ labeled amino acids (CIL) except for cysteine (^{15}N labelled) and tryptophan (unlabelled). CTLA-4ex contains no tryptophan. Amino acids were added at concentrations equivalent to alpha-MEM media (Gibco); the media also contained ^{13}C labelled glucose (2 g l^{-1}) and ^{13}C labelled pyruvate (110 mg l^{-1}). Cells were innoculated into cell factories (NUNC) and allowed to grow for 1 week, at which point the media was harvested and the CTLA4Ig was processed as described above. Approximately 7 mg of $^{15}N/^{13}C$-labeled, partially deglycosylated CTLA-4 was obtained from 3 l of culture. This sample was very stable, lasting over 9

months at 30 °C and able to undergo multiple exchanges from H_2O to D_2O.

Structure determination. NMR experiments were collected at 30 °C on a Varian UnityPlus 600 spectrometer, using a single, 0.7 mM, ^{13}C-^{15}N labelled sample of CTLA-4ex. Sequential resonance assignments were made through analysis of the following three dimensional experiments: HNCO, HNCA, HN(CO)CA, HNCACB, CBCA(CO)NH, HBHA(CO)NH, CC-TOCSY(CO)NH, ^{15}N-separated TOCSY, and HCCH-TOCSY[19]. Interproton distance restraints were derived primarily from the cross-peak intensities of the 3D ^{15}N-separated and 3D ^{13}C-separated NOESY spectra[19] acquired with a mixing time of 80 ms. In addition, a 4D $^{13}C/^{13}C$-separated NOESY spectrum[19] (mixing time = 60 ms) was used to resolve assignment ambiguities, particular for NOEs arising from methyl resonances. Restraint bounds were generated by setting the lower bound equal to the sum of the van der Waal's radii (1.8 Å) and by setting the upper bound equal to 1.3 times the calculated target distance. Φ angle restraints were derived from $^3J_{HN,H\alpha}$ values obtained by analysis of a gradient-enhanced (GE) version of the HSQC-J-modulated [^{15}N,^1H]-COSY experiment[20]. Observed J values were corrected for the effect of relaxation due to $T_{1sel}(^1H\alpha)$[21]. Restraint ranges for Φ were set to -120° +/- 40° (for $^3J_{HN,H\alpha} \geq 8.0$ Hz) and -60° +/- 40° (for $^3J_{HN,H\alpha} < 5.6$ Hz and when the short range NOE data could unambiguously discern between +60° and -60°). Stereospecific valine γ-methyl assignments and restraints on χ_1 for isoleucine, valine and threonine were based on the values of $J_{NC}{}^{\gamma}$ and $JC'C^{\gamma}$ obtained from the 2D {^{15}N} and {^{13}C} spin-echo difference, constant-time HSQC experiments[22–23] and relative intraresidue NOE intensities. The chemical shifts of $^{13}C\beta$ and $^{13}C\gamma$ resonances of Pro 103, 34.6 and 24.6 p.p.m. respectively, indicate that Pro 103 is in the *cis* conformation. The conformation of the loop is well-determined, despite the fact that no resonance assignments were obtained for either Pro 101 or Pro 102. Strong NOEs are observed between the ε-methyl of Met 99 and the aromatic protons of Tyr 104. Additional NOEs are observed between the back bone and side chain protons of Leu 98–Tyr 100 and Tyr 104–Leu 106 .

Structures were generated using a combined distance geometry/restrained dynamic simulated annealing approach in X-PLOR 3.1[24–25], which had been modified to include conformational database refinement[26]. Final structure calculations were based on 938 interproton distance restraints [372 intraresidue restraints, 188 sequential restraints, 57 medium-range restraints ($2 \leq |i-j| \leq 4$), and 277 long-range restraints ($|i-j| > 4$), 23 carbohydrate–protein distance restraints, and 21 intracarbohydrate restraints]. These were supplemented with 63 torsion angle restraints [41 Φ and 22 χ_1], 62 restraints for 31 hydrogen bonds associated with slowly exchanging backbone amide protons, and two disulphide bond restraints. In addition, because the relative intensities of intrasugar NOEs indicated these sugars were predominantly in their lowest energy chair conformations, the sugars were forced into these conformations with torsion angle restraints, and the corresponding intrasugar NOE restraints were excluded. The final structures were analyzed for best fit to the experimental NMR restraints and the overall energy. As the energy did not vary significantly among the structures, the twenty structures with the lowest residual experimental restraint violations were chosen to represent the ensemble of solution conformations for CTLA-4ex. Coordinates have deposited in the Brookhaven Protein Data Bank (accession code: 1AH1).

Mutagenesis. Site directed mutagenesis of CTLA4Ig was performed using PCR forward mutagenic primers as previously described[14]. All mutations were verified by DNA sequencing and mutant proteins were expressed in COS cells[14]. The structural integrity of each mutant was confirmed by testing its ability to bind a panel of anti-CTLA-4 monoclonal antibodies; all molecules bound monoclonal antibodies similar to wild type CTLA4Ig. Binding of graded concentrations of each protein to immobilized CD80Ig and CD86Ig proteins was measured and compared to wild type CTLA4Ig[14]. The activities relative to wild type CTLA4Ig for binding of each new mutant to CD80Ig and CD86Ig, respectively, were: wt, 100% and 100%; N78D, ~20%, ~20%; N111D, ~100%, ~100%; E31S, <1% and <1%; R33S, 28% and <1%; T35S, 100% and 100%; L37S, 100% and 100%; E46S, 61% and 14%; T51S, 100% and 100%; and K95S, 14% and 16%.

William J. Metzler[1], Jürgen Bajorath[3], William Fenderson[2], Shyh-Yu Shaw[2], Keith L. Constantine[1], Joseph Naemura[4], Gina Leytze[4], Robert J. Peach[4], Thomas B. Lavoie[2], Luciano Mueller[1] and Peter S. Linsley[4]

[1]Departments of Macromolecular NMR, [2]Peptide and Protein Research, Bristol-Myers Squibb Pharmaceutical Research Institute, PO Box 4000, Princeton, New Jersey 08543-4000, USA. [3]Departments of Inflammation, and [4]Immunomodulation, Bristol-Myers Squibb Pharmaceutical Research Institute, 3005 First Avenue, Seattle, Washington 98121, USA.

Correspondence should be addressed to W.J.M. *email: metzler@laplaya.bms.com*

Acknowledgements
We thank the Bristol-Myers Squibb Bioprocess Research Group for production of CTLA4Ig, B.T. Farmer for assistance with NMR techniques, M. Friedrichs for computational support, T. Skinner for technical assistance, M. Hail and B. Warrack for mass spectral analysis, Y. Wu for determination of carbohydrate composition, and S. Sheriff, G.R. Matsueda and H. Einspahr and especialy G.R. Matueda for insights and discussions.

Received 25 February; accepted 16 May 1997.

1. June, C. H., Bluestone, J.A., Nadler, L.M. & Thompson, C.B. *Immunol. Today* **15**, 321–332 (1994).
2. Walunas, T.L. et al. *Immunity* **1**, 405–413 (1994).
3. Krummel, M.F. & Allison, J.P. *J. Exp. Med.* **182**, 459–465 (1995).
4. Kearney, E.R. et al. *J. Immunol.* **155**, 1032–1036 (1995).
5. Leach, D. R., Krummel, M. F. & Allison, J. P. *Science* **271**, 1734–1736 (1996).
6. P. Waterhouse, et al., *Science* **270**, 985–988 (1995).
7. Tivol, E. A. et al. *Immunity* **3**, 541–547 (1995).
8. Greene, J. L. et al., *J. Biol. Chem.* **271**, 26762–26771 (1996).
9. Linsley, P.S. et al. *J. Biol. Chem.* **270**, 15417–15424 (1995).
10. Linsley, P.S., Brady, W., Urnes, M., Grosmaire, L. S., Damle, N. K. & Ledbetter, J. A. *J. Exp. Med.* **174**, 561–570 (1991).
11. Finck, B.K. , Linsley, P.S. & Wofsy, D. *Science* **265**, 1225–1227 (1994).
12. Wyss, D.F., et al. *Science* **269**, 1273–1278 (1995).
13. Chothia, C., Novotny, J., Bruccoleri, R., & Karplus, M. *J. Mol. Biol.* **186**, 651–663 (1985).
14. Peach, R.J., et al. *J. Exp. Med.* **180**, 2049–2058 (1994).
15. Morton et al., *J. Immunol.* **156**, 1047–1054 (1996).
16. Truneh, et al., *Mol. Immunol.* **33**, 321-334 (1996).
17. Kariv, K., Truneh, A. & Sweet, R. W. *J. Immunol.* **157**, 29–38 (1996).
18. Harris et al., *J. Exp. Med.* **In the press**
19. Clore, G. M. & Gronenborn, A. M. *Meth. Enzymol.* **239**, 349–363 (1994).
20. Billiter, M., Neri, D., Otting, G., Qian, Y., & Wuthrich, K. *J. Biomol. NMR* **2**, 257–274.
21. Kuboniwa, H., Grzeslek, S., Delaglio, F., Bax, A. *J. Biomol. NMR* **4**, 871–878 (1994).
22. Bax, A., Max, D. & Zax, D. *J. Amer. Chem. Soc.* **114**, 6923–6925 (1992).
23. Vuister, G. W., Wang, A. C. & Bax, A. *J. Am. Chem. Soc.* **115**, 5334–5335 (1993).
24. AT Brunger, XPLOR Version 3.1: A system for X-ray Crystallography and NMR (Yale Univ. Press, New Haven, CT) 1993.
25. Nilges, M., Clore, G.M. & Gronenborn, A.M. *.FEBS Lett.* **229**, 317–324 (1988).
26. Kuszewski, J., Gronenborn, A.M. & Clore, G.M. *Prot. Sci.* **5**, 1067–1077 (1996).
27. M Carson, Ribbons 2.0. *J. Appl. Cryst.* **24**, 958–961 (1991).